Optics Letters

Compact and adjustable compensator for AOD spatial and temporal dispersion using off-the-shelf components

Akihiro Yamaguchi, Doycho Karagyozov, and Marc H. Gershow*

Department of Physics and Center for Soft Matter Research, New York University, New York, New York 10003, USA
**Corresponding author: marc.gershow@nyu.edu*

Received 15 January 2021; revised 25 February 2021; accepted 26 February 2021; posted 26 February 2021 (Doc. ID 419682); published 23 March 2021

Random access multiphoton microscopy using two orthogonal acousto-optic deflectors (AODs) allows sampling only particular regions of interest within a plane, greatly speeding up the sampling rate. AODs introduce spatial and temporal dispersions, which distort the point spread function and decrease the peak intensity of the pulse. Both of these effects can be compensated for with a single dispersive element placed a distance before the AODs. An additional acousto-optic modulator, a custom cut prism, and a standard prism used with additional cylindrical optics have been demonstrated. All of these introduce additional cost or complexity and require an extended path length to achieve the needed negative group delay dispersion (GDD). By introducing a telescope between a transmission grating and the AODs, we correct for spatial and temporal dispersions in a compact design using only off-the-shelf components, and we show that the GDD can be tuned by translation of the telescope without adjustment of any other elements.

https://doi.org/10.1364/OL.419682

Multiphoton laser scanning microscopy with acousto-optic deflectors (AODs) involves no mechanical movement and provides a fast scanning rate with constant point-to-point transition time, high precision, and stability. 2D [1–6] and 3D [7–10] random access multiphoton (RAMP) microscopes have been developed using two and four AODs, respectively. These AODs introduce angular and temporal dispersions, which, if not corrected, result in pulse broadening and beam distortion, degrading the signal intensity and image resolution.

Four AODs allow for 3D random access positioning, but dwell time is limited for points far from the natural objective focus, the setup is complex, and the total power throughput is low [7,11]. Angular dispersion is internally compensated for; temporal dispersion is separately compensated for by an external unit, which can be quite large (>1 m in [7]).

Two orthogonal AODs can position a stationary [1–4,6] or locally moving [5] focal spot within a plane. Other methods can be used for axial focusing, or, using a laser with inter-pulse intervals comparable to the AOD acoustic access time, 3D positioning can be achieved directly [12]. In these setups, a single prism or additional acousto-optic device can correct for both spatial and temporal dispersions [2,4–6,12–15]. The element must be chosen to exactly cancel the angular dispersion introduced by the AODs, often requiring custom fabrication.

In this Letter, we demonstrate a simple, compact, and efficient scheme employing only off-the-shelf components—a transmission grating and a telescope—to compensate for the angular and temporal dispersions of two orthogonal AODs. This system shortens the optical train and provides new ability to tune the group delay dispersion (GDD) by translation of the telescope along the optical axis without adjustment of any other component.

If light of wavelength λ and bandwidth $\Delta\lambda$ is incident on an AOD with acoustic velocity v_a driven by sound with a frequency ν, then the angle of deflection θ_d, the spread in angles $\Delta\theta$, and the spatial dispersion (Δx) under an objective of focal length f_o are

$$\theta_d = \frac{\nu\lambda}{v_a}, \tag{1}$$

$$\Delta\theta = \frac{\partial\theta}{\partial\lambda}\Delta\lambda = \frac{\nu}{v_a}\Delta\lambda = \theta_d\frac{\Delta\lambda}{\lambda}, \tag{2}$$

$$\Delta x = f_o\Delta\theta = f_o\theta_d\frac{\Delta\lambda}{\lambda}. \tag{3}$$

AODs also contribute GDD, which broadens a Gaussian pulse with FWHM τ_0 according to [14]

$$\tau = \tau_0\sqrt{1+\left(\frac{4\ln 2}{\tau_0^2}\cdot \mathrm{GDD}\right)^2}. \tag{4}$$

In typical systems with large AODs fabricated from highly dispersive TeO_2 [2,14,15], the spread of the focal spot Δx is much larger than the diffraction limited spot size, and pulses are stretched by $5-10\times$. These effects degrade imaging performance and reduce the efficiency of two-photon excitation.

To remedy angular dispersion, a dispersive element is placed in front of the AOD, oriented so that its dispersion cancels that of the AOD at θ_c, the central deflection angle. Two orthogonally

oriented AODs can be compensated for by a single element tilted between the AODs' deflection planes [13,15]. This also corrects for temporal dispersion by creating a region of *negative* group velocity dispersion (GVD) between the element and AOD [16]:

$$\mathrm{GVD} = -\frac{\lambda^3}{2\pi c^2}\left(\frac{\partial\theta}{\partial\lambda}\right)^2. \tag{5}$$

The beam is allowed to travel a distance L in the region of negative GVD to cancel the AOD's positive GDD, calculated by multiplying $\mathrm{GVD}_{\mathrm{AOD}}$, the AOD's GVD by its length L_{AOD}. As $\frac{\partial\theta}{\partial\lambda}$ is chosen to cancel the AOD's angular dispersion at θ_c, the central deflection angle, L is a property of the AOD:

$$L = \mathrm{GVD}_{\mathrm{AOD}} L_{\mathrm{AOD}} \theta_c^{-2}\left(\frac{2\pi c^2}{\lambda}\right). \tag{6}$$

For $\lambda = 1$ μm, a TeO_2 deflector with GVD ≈ 4000 fs^2/cm, and $\theta_c = 70$ mrad, this is 46 cm of free space per centimeter of AOD thickness for a single AOD. The same distance is required if two identical orthogonal AODs are used because L_{AOD} doubles, while θ_c increases by a factor of $\sqrt{2}$.

The compensating element can be a prism [2,4,6,13,15,17] or another acousto-optic device [1,5,12,14,15,18]. If a prism is used, it must be oriented at the angle of minimum deviation with the angle of incidence at the Brewster angle or the beam will be distorted and light lost to reflection. This requires custom fabrication [4,17]. Otherwise, the beam shape can be corrected with cylindrical optics [2], but Fresnel losses remain. An additional AOD or AOM increases the cost and complexity of the system, and the GDD that must be compensated for. We are not aware of any experimental realizations using a fixed diffraction grating [15]. In all realizations, fine-tuning the GDD requires substantial effort and precise realignment to adjust the distance between the compensating element and the AODs [14,17].

A Keplerian telescope (KT) beam expander with two lenses of focal lengths f_1 and f_2 that share a common focus magnifies the size of an incoming beam by an amount $M = f_2/f_1$ while decreasing the angular divergence by a factor $1/M$. If we place a KT after the dispersive compensating element [Fig. 1(a)], the angular dispersion of the AODs is compensated for if [19]

$$\left(\frac{\partial\theta}{\partial\lambda}\right)_{\mathrm{element}} = M\cdot\left(\frac{\partial\theta}{\partial\lambda}\right)_{\mathrm{AODs}}. \tag{7}$$

Combinations of achromatic off-the-shelf lenses can be chosen for any M, allowing flexibility in the compensating element.

This geometry has an additional advantage in temporal dispersion compensation. The space between the compensating element and the first AOD is partitioned into three regions, each with different GDDs [16] [Fig. 1(b)]. In region 2, between the focal planes of the KT, due to the principal of least time, the total GDD is zero. In regions 1 (between the grating and front telescope focus, a distance L_1) and 3 (between the rear telescope focus and the AOD, a distance L_3), the GVD is proportional to the square of the angular divergence [Eq. (5)]. In region 3, by design, the angular dispersion cancels that of the AOD: $(\frac{\partial\theta}{\partial\lambda})_3 = -\frac{\theta_c}{\lambda}$, while in region 1, it is $-M$ times larger. The total GDD is therefore

$$\mathrm{GDD} = -\frac{\lambda^3}{2\pi c^2}\left(\frac{\theta_c}{\lambda}\right)^2 (M^2\cdot L_1 + L_3). \tag{8}$$

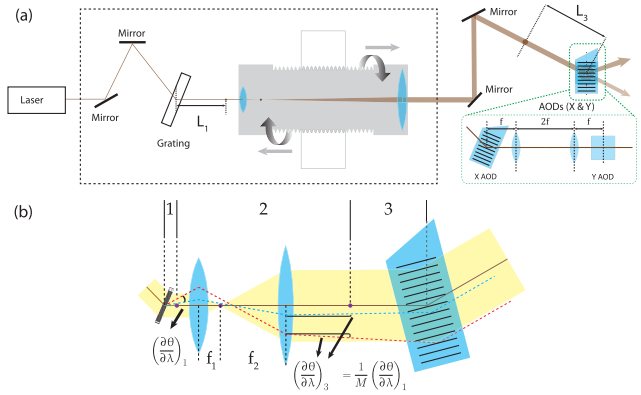

Fig. 1. Simultaneous angular and adjustable temporal dispersion compensation with a fixed grating and beam expander. (a) Optical path: a pulsed laser beam is diffracted at the Bragg angle from a volume phase holographic grating and expanded by a telescope before being directed into two orthogonally oriented AODs placed in conjugate planes by a 4f relay. The telescope is constructed in a lens tube and can be translated by rotation of the tube within its mount. The elements indicated with a dashed box are mounted at 45 deg to the optical table. (b) Three regions contribute differently to the total GDD. 1 (between the grating and telescope front focus): high angular dispersion and a large negative GVD. 2 (between the focal planes of the telescope): zero net GDD. 3 (between the telescope rear focus and the AOD): the beam diameter is larger and the angular dispersion smaller by a factor of $M = f_2/f_1$. Blue and red dashed lines schematize paths of short and long wavelength components, respectively.

Because of the high dispersion in region 1, the total distance $L = L_1 + L_3 + 2(f_1 + f_2)$ can be much shorter than without the KT, allowing even for the size of the telescope. Further, the partition between L_1 and L_3 can be adjusted by translating the KT along the optical axis, allowing post-assembly tuning of the total negative GDD. Translation of the whole telescope towards the AOD by ΔL_1 increases L_1 and decreases L_3 by ΔL_1, so

$$\Delta\mathrm{GDD} = -\frac{\lambda^3}{2\pi c^2}\left(\frac{\theta_c}{\lambda}\right)^2 (M^2 - 1)\Delta L_1. \tag{9}$$

To demonstrate these ideas experimentally, we used as a light source a Chameleon Ultra II laser that delivered 125 fs duration (FWHM) pulses at a central wavelength of $\lambda = 970$ nm. A prism based precompensator (Chameleon Precomp) immediately after the laser was set to zero GDD but due to imperfect adjustment contributed some initial GDD; following the precomp, the pulse width was 147 fs. We used two orthogonally mounted AODs (Gooch & Housego, Model: MD050-9S2V47-3-6.5DEG-WAA-X and MD050-9S2V47-3-6.5DEG-WAA-Y) made of TeO_2. The AODs were separated by a 4f relay to reside in conjugate optical planes. At the central operating frequency of 50 MHz and a wavelength of 970 nm, the angular deflection of each AOD was 4.28°. The total angular dispersion to be compensated for was therefore 6.05°/μm.

The AOD acoustic aperture was 9 mm, and at $\lambda = 970$ nm, the range of deflection angles was 2.57°, implying a field of view (FOV) of ±100 μm if the AODs were relayed onto a NA 1 objective.

For the fixed compensating element, we chose a volume phase holographic transmission grating (Wasatch Photonics,

800 lp/mm pitch, $d = 1.25$ μm, diffraction efficiency, $\eta > 90\%$ at 1030 nm, 25 × 35 mm, 6 mm thick), mounted at 45° to the table. The grating is designed to be used at the Bragg angle (22.83°), generating an angular dispersion of 49.73°/μm at a wavelength of 970 nm. To match the angular dispersion of the grating to the AODs, we needed to expand the beam by $M = 8.23$.

We created a KT with 8× beam expansion from two standard achromatic lenses (Thorlabs, AC254-080-B-ML and AC080-010-B-ML) assembled inside a SM1 lens tube (Thorlabs). The lens tube was mounted in a threaded housing, so the telescope could be axially translated by rotating the lens tube [Fig. 1(a)]. The total path length between the grating and the first AOD was 25 cm. Spatial chirp elongated the beam along one axis by 10% at the AODs (see Supplement 1).

The lenses, lens tubes, optical mounts, and fold mirrors were ordered from stock at Thorlabs, and the grating from stock at Wasatch. All components of the compensating system were off the shelf; no custom fabrication or special orders were required.

To characterize the angular dispersion, we focused the post AOD beam through a 100 mm focal length lens onto a CMOS sensor (Basler, Model: acA1920-150um) while adjusting the driving frequency to the x and y AODs in 5 MHz increments.

To characterize the temporal dispersion, we measured the pulse width following the AODs using an autocorrelator with a separate delay line and nonlinear detector (FEMTOCHROME Research, Inc. Model: FR-103TPM). Signals were digitized with an oscilloscope (Tektronix TDS2024C) and analyzed in MATLAB. The FWHM of the light pulse was determined by multiplying the FWHM of the autocorrelator trace by 0.65. Each data point and error bar in Fig. 3 represents the mean and standard error of the mean following at least six independent placements of the KT at that position.

When a Gaussian pulse of initial FWHM τ_0 experiences GDD, the pulse is broadened according to Eq. (4).

We measured τ, the laser output pulse width, to be 146.7 ± 0.2 fs immediately prior to the compensation unit. Following the AODs but without dispersion compensation, this pulse was broadened to 625.1 ± 10.4 fs. Without compensation, the beam retained angular divergence, so the pulse width depended on the position of the measurement; this value was obtained as close to the AODs as practical. We then inserted the compensation unit and adjusted the position of the KT to minimize the pulse width. Following this adjustment, the pulse

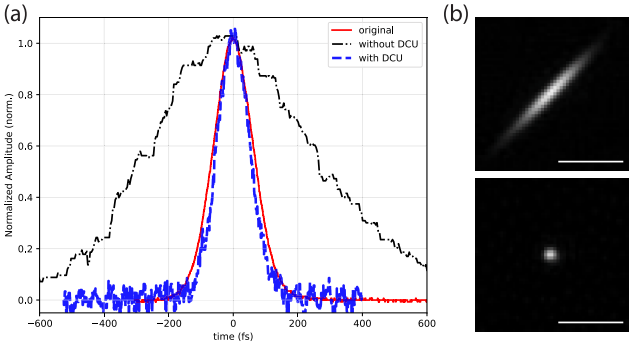

Fig. 2. Temporal and spatial dispersion. (a) Normalized correlation waveforms from output of the laser source (solid red line, 147 fs) after the 2D AOD without grating compensation (solid black line, 625 fs) and with grating compensation (blue dashed line, 125 fs). (b) Angular dispersion of the beam without (top) and with (bottom) the compensating grating; measured at $\nu_x = \nu_y = 50$ MHz. Scale bar 1 mrad.

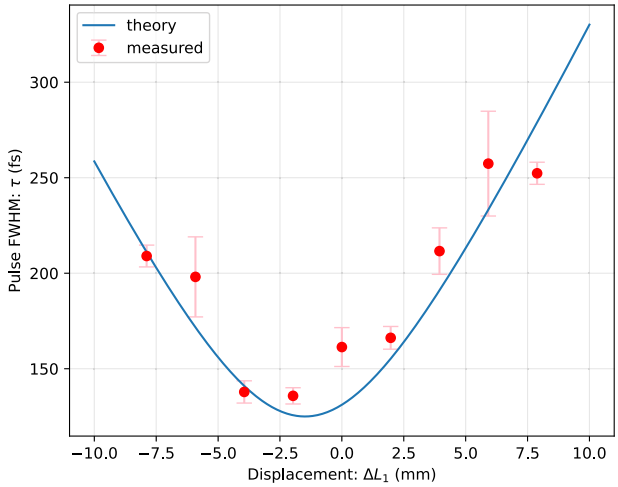

Fig. 3. Pulse width versus telescope translation data, and error bars represent mean and s.e.m. for at least six independent measurements. Curve represents the prediction of Eq. (12) with L_0, the location of the minimum, the only free parameter. $\Delta L_1 = 0$ represents the location of the KT after initial adjustment to near the apparent minimum pulse width.

width was 125.3 ± 1.7 fs, indicating the compensation unit is capable of cancelling the GDD associated with the AODs and other components in the optical path [Fig. 2(a)].

Figure S1 shows the beam spots without and with dispersion compensation. The beam was deflected to an array of positions in the FOV by the 2D AOD scanner. Without compensation, the spots were elliptical (Fig. S1a) and the ratio of long axis to short axis was 6.9 ± 0.7 at the center frequency [Fig. 2(b)]. With compensation, the spots reverted to circular (Fig. S1b), with a ratio of 1.2 ± 0.1 at the center frequency [Fig. 2(b)]. We used a telescope with magnification of eight rather than the calculated 8.23, so perfect angular compensation was achieved at 51.4 MHz rather than 50 MHz.

The optical throughput was 85% following the grating and 22% following the entire scan unit [all components in Fig. 1(a)].

Translation of the KT away from the diffraction grating by an amount ΔL_1 creates additional negative GDD according to

$$\Delta\mathrm{GDD} = -\frac{2\lambda}{\pi c^2} \cdot \tan^2\theta_B \left(1 - \frac{1}{M^2}\right) \Delta L_1 \tag{10}$$

$$= -1200 \frac{\mathrm{fs}^2}{\mathrm{mm}} \Delta L_1 (\text{our system}). \tag{11}$$

To test this prediction, we first adjusted the KT to minimize the pulse width after the AODs. We then translated the KT away from this minimum while measuring the pulse width. Because the pulse width is insensitive to translation of the KT near the minimum, we allowed for the possibility that the true minimum was displaced from our initial estimate and fit the pulse widths to the model [combining Eq. (4) and Eq. (10)]:

$$\tau(L_1) = \tau_0 \sqrt{1 + \left(\frac{4\ln 2}{\tau_0^2} \frac{2\lambda}{\pi c^2} \tan^2\theta_B \left(1 - \frac{1}{M^2}\right) \cdot (L_1 - L_0)\right)^2}$$

$$= 125\ \mathrm{fs} \sqrt{1 + \left(.213 \frac{L_1 - L_0}{\mathrm{mm}}\right)^2}, \tag{12}$$

where L_0, a fit parameter, represents the location at which the GDD is best compensated for, and 125 fs, the shortest pulse we measured with any amount of compensation, was taken to be the bandwidth limited pulse FWHM duration.

Figure 3 shows the measured and predicted pulse widths as a function of the translation of the KT. Note that the only fit parameter in the prediction is the location of the minimum.

Angular and temporal dispersion of two orthogonally oriented AODs can be compensated for by a single optical element placed upstream of the AODs. In previous work, the beam was expanded prior to the compensating element, which was chosen to exactly match the angular dispersion of the AODs, placing significant constraints on the choice of compensating optical elements.

Here we have shown that a simple reordering of the sequence of the beam expanding telescope, compensating element, and AODs provides several advantages.

1. The angular dispersions of any off-the-shelf compensating element and AODs can be matched by selecting off-the-shelf lenses to create the appropriate expansion factor (M). A large M allows the use of small aperture compensating elements and gratings with large angular dispersion.
2. Before the telescope, the negative GVD is larger by a factor of M^2. A shorter path achieves the required negative GDD.
3. Translation of the telescope allows simple tuning of the GDD over a large range.

In this work, we used a single beam expander to match the angular dispersion of the fixed grating to the AODs and to expand the laser beam to fill the acoustic aperture of the AODs. Often it will be possible to select a grating to achieve this happy coincidence, but otherwise, a second telescope may be placed before the grating.

Unlike prism-based systems, design choices are relatively insensitive to the central wavelength of the laser, and the system is easily reconfigured to accommodate different wavelengths—only tilt adjustments are needed to compensate for changing diffraction angles. Prisms allow for compensation of third order disperion (TOD), but residual angular dispersion ultimately limits pulse bandwidth, and our compensator faces the same limitations on pulse duration as systems without a telescope (see Supplement 1).

In our setup, typical for random access microscopy, the additional GDD achieved by translating the telescope ($1{,}200\ \mathrm{fs}^2/\mathrm{mm}$) is convenient. Large adjustments are made with modest translations ($10{,}000\ \mathrm{fs}^2$ with <1 cm of translation) but fine hand adjustment is still straightforward. This method of GDD adjustment can be applied to other compensators by placing two telescopes back to back in the negative GVD region and translating one with respect to the other.

In summary, a single high-efficiency transmission grating combined with a beam expander can be used to compensate for angular dispersion of AODs and create a compact easily tuned source of negative GDD. This has applications in ultrashort pulse steering and multiphoton microscopy.

Funding. National Science Foundation (1455015); National Institutes of Health (1DP2EB022359).

Disclosures. The authors declare no conflicts of interest.

Supplemental document. See Supplement 1 for supporting content.

REFERENCES

1. R. Salomé, Y. Kremer, S. Dieudonné, J. F. Léger, O. Krichevsky, C. Wyart, D. Chatenay, and L. Bourdieu, J. Neurosci. Methods **154**, 161 (2006).
2. B. F. Grewe, D. Langer, H. Kasper, B. M. Kampa, and F. Helmchen, Nat. Methods **7**, 399 (2010).
3. D. Vučinić and T. J. Sejnowski, PLoS ONE **2**, e699 (2007).
4. R. Jiang, Z. Zhou, X. Lv, and S. Zeng, Rev. Sci. Instrum. **83**, 043709 (2012).
5. V. Villette, M. Chavarha, I. K. Dimov, J. Bradley, L. Pradhan, B. Mathieu, S. W. Evans, S. Chamberland, D. Shi, R. Yang, B. B. Kim, A. Ayon, A. Jalil, F. St-Pierre, M. J. Schnitzer, G. Bi, K. Toth, J. Ding, S. Dieudonné, and M. Z. Lin, Cell **179**, 1590 (2019).
6. Y. Shao, W. Qin, H. Liu, J. Qu, X. Peng, H. Niu, and B. Z. Gao, Opt. Lett. **37**, 2532 (2012).
7. G. Katona, G. Szalay, P. Maák, A. Kaszás, M. Veress, D. Hillier, B. Chiovini, E. S. Vizi, B. Roska, and B. Rózsa, Nat. Methods **9**, 201 (2012).
8. G. Duemani Reddy, K. Kelleher, R. Fink, and P. Saggau, Nat. Neurosci. **11**, 713 (2008).
9. K. M. N. S. Nadella, H. Roš, C. Baragli, V. A. Griffiths, G. Konstantinou, T. Koimtzis, G. J. Evans, P. A. Kirkby, and R. A. Silver, Nat. Methods **13**, 1001 (2016).
10. V. A. Griffiths, A. M. Valera, J. Y. Lau, H. Roš, T. J. Younts, B. Marin, C. Baragli, D. Coyle, G. J. Evans, G. Konstantinou, T. Koimtzis, K. M. N. S. Nadella, S. A. Punde, P. A. Kirkby, I. H. Bianco, and R. A. Silver, Nat. Methods **17**, 741 (2020).
11. P. A. Kirkby, K. M. N. S. Nadella, and R. A. Silver, Opt. Express **18**, 13720 (2010).
12. W. Akemann, J.-F. Léger, C. Ventalon, B. Mathieu, S. Dieudonné, and L. Bourdieu, Opt. Express **23**, 28191 (2015).
13. S. Zeng, X. Lv, C. Zhan, W. R. Chen, W. Xiong, S. L. Jacques, and Q. Luo, Opt. Lett. **31**, 1091 (2006).
14. Y. Kremer, J.-F. Léger, R. Lapole, N. Honnorat, Y. Candela, S. Dieudonné, and L. Bourdieu, Opt. Express **16**, 10066 (2008).
15. S. Zeng, X. Lv, K. Bi, C. Zhan, D. Li, W. R. Chen, W. Xiong, S. L. Jacques, and Q. Luo, J. Biomed. Opt. **12**, 024015 (2007).
16. O. E. Martinez, J. P. Gordon, and R. L. Fork, J. Opt. Soc. Am. A **1**, 1003 (1984).
17. B. F. Grewe and F. Helmchen, *High-Speed Two-Photon Calcium Imaging of Neuronal Population Activity Using Acousto-Optic Deflectors* (Cold Spring Harbor Laboratory, 2014).
18. V. Iyer, B. E. Losavio, and P. Saggau, J. Biomed. Opt. **8**, 460 (2003).
19. O. E. Martinez, Opt. Commun. **83**, 117 (1991).